Oxygen Mobility in CeO2 and CexZr(1−x)O2 Compounds: Study by CO Transient Oxidation and 18O/16O Isotopic Exchange

ARTICLE · DECEMBER 1999

DOI: 10.1021/jp991270a

4 AUTHORS, INCLUDING:

Claude Descorme
French National Centre for Scientific Research
124 PUBLICATIONS **2,388** CITATIONS
SEE PROFILE

Daniel Duprez
Université de Poitiers
311 PUBLICATIONS **7,244** CITATIONS
SEE PROFILE

Oxygen Mobility in CeO_2 and $Ce_xZr_{(1-x)}O_2$ Compounds: Study by CO Transient Oxidation and $^{18}O/^{16}O$ Isotopic Exchange

Y. Madier,[†] C. Descorme,*[,†] A. M. Le Govic,[‡] and D. Duprez[†]

Laboratoire de Catalyse en Chimie Organique (LACCO), UMR CNRS 6503, Université de Poitiers, 40, avenue du Recteur Pineau, 86022 Poitiers Cedex, France, and Centre de Recherche d'Aubervilliers (CRA), Rhodia, 52, rue de la Haie Coq, 93308 Aubervilliers Cedex, France

Received: April 19, 1999; In Final Form: September 22, 1999

Cerium−zirconium mixed oxides ($Ce_xZr_{(1-x)}O_2$), precalcined at 900 °C in dry air, were supplied by Rhodia Terres Rares as monophasic solid solutions. Introduction of some zirconium atoms in the ceria lattice by isomorphous substitution clearly influences the final properties of these materials as long as the cubic structure of ceria is maintained. Modifications in oxygen storage capacity (OSC measurements), redox properties (CO TPR), and oxygen exchange processes (TPIE) were studied. $Ce_{0.63}Zr_{0.37}O_2$ was shown to have the most promising properties with the largest OSC at 400 °C and the highest reactivity in O_2 exchange. All mixed oxides are able to exchange very large amounts of oxygen compared to ceria, implying the participation of bulk oxygen. Furthermore, on $Ce_xZr_{(1-x)}O_2$ samples, oxygen is predominantly exchanged via a multiple heteroexchange mechanism involving surface dioxygen species as superoxides or peroxides.

Introduction

Three-way catalysts (TWC) simultaneously have to oxidize CO and hydrocarbons (HC) to CO_2 and reduce NO_x to N_2. Both oxidation and reduction reactions may take place at the same time if a stoichiometric mixture is employed. For that reason the ratio of oxidants (O_2, NO_x) to reductants (H_2, CO, HC) should be maintained close to unity. This domain, where both CO, HC, and NO_x conversions are optimum, is called the operating window. To enlarge this operating window and improve the catalyst performances during oscillations around the stoichiometry, ceria is systematically added to TWC. According to its redox properties, with a fast Ce^{4+}/Ce^{3+} balance, ceria can store O_2 during an oxygen-rich phase[1] and feed the noble metal with oxygen when the O_2 partial pressure decreases. This specific property of ceria is commonly studied by measuring the oxygen storage capacity (OSC) of the modified materials.

Nowadays, ceria tends to be replaced by $Ce_xZr_{(1-x)}O_2$ mixed oxides. These new oxides have both better thermal stability and larger OSC.[2−9] High thermal stability is an essential requirement for these materials employed as supports in automotive converters. In fact, TWC can meet temperatures up to 1000 °C. Numerous studies have been devoted to the investigation of structural,[10−19] surface,[20−22] and redox properties[3,4,6,23−25] of these materials.

In this paper, OSC and redox properties of CeO_2, ZrO_2, and $Ce_xZr_{(1-x)}O_2$ materials prepared by Rhodia are investigated, focusing on the correlation with $^{16}O/^{18}O$ isotopic exchange measurements.[26−27]

Experimental Section

Materials. Cerium−zirconium mixed oxides with $Ce_xZr_{(1-x)}O_2$ formula, x ranging from 0 to 1, were prepared by Rhodia Terres Rares (La Rochelle, France). Mixed oxide solid solutions are obtained by isomorphous substitution of Ce^{4+} cations (ionic radius 0.97 Å) with Zr^{4+} cations (ionic radius 0.84 Å). This substitution involves a decrease of the cell volume and the creation of structural defects. These defects play a crucial role in determining the redox properties of these solids.

Six oxides, with $x = 1$, 0.68, 0.63, 0.50, 0.15, and 0, are under study. These materials were calcined in a muffle furnace at 900 °C for 6 h in order to work on stabilized samples.

Characterization. *Structural Studies.* Surface areas were measured by N_2 adsorption at −196 °C (single-point method) using a Micromeritics Flowsorb II.

Powder X-ray diffraction patterns were collected on a Siemens D500 diffractometer using Cu Kα radiation (λ = 1.5406 Å). Crystalline phases were identified by comparison with the ICDD files. To calculate the integrated width (β), diffractograms were simulated using Profile (Socabim, France). The best fit was obtained when assuming a Gaussian profile for the diffraction peaks. Calculated β values are corrected from the instrumental width determined using a silicium reference (SRM640a from NBS). An average crystallite size ($\bar{D}$) was then calculated from the Debye−Scherrer relation using peaks (111), (200), and (220) for ceria and cerium-rich mixed oxides (cubic structure), peaks (101), (110), (002), (200), (112), (211), and (103) for samples with tetragonal structure, and peaks (−111) and (111) for zirconia. Experimental lattice parameters were finally calculated using a simulation program called U-FIT. This cell parameter refinement program was designed by M. Evain (IMN Nantes, France, 1992).

Structural properties of $Ce_xZr_{(1-x)}O_2$ samples are summarized in Table 1.

Surface Oxygen Reactivity. Carbon monoxide oxidation on cerium−zirconium mixed oxides was studied by the way of three different methods of characterization: temperature-programmed reduction (TPR), oxygen storage capacity (OSC) measurements, and study of $C^{16}O$ oxidation and exchange on ^{18}O-exchanged oxides.

* To whom correspondence should be addressed. Telephone: +335 49 45 39 97. Fax: +335 49 45 34 99. E-mail: claude.descorme@campus.univ-poitiers.fr.

[†] Université de Poitiers.

[‡] Rhodia.

10.1021/jp991270a CCC: $18.00
Published on Web 11/23/1999

TABLE 1: Structural Properties of $Ce_xZr_{(1-x)}O_2$ Solid Solutions

oxides	surface area[a] ($m^2\ g^{-1}$)	stucture (ICDD file numbers)	lattice parameter[b] (Å)	crystallite size (Å)
CeO_2	25	cubic (43-1002)	$a = 5.403$	260
$Ce_{0.68}Zr_{0.32}O_2$	40	cubic	$a = 5.323$	110
$Ce_{0.63}Zr_{0.37}0_2$	40	cubic (38-1439)	$a = 5.310$	110
$Ce_{0.50}Zr_{0.50}O_2$	45	tetragonal (38-1436)	$a = b = 3.724$ $c = 5.269$	100
$Ce_{0.15}Zr_{0.85}O_2$	25	tetragonal	$a = b = 3.637$ $c = 5.239$	190
ZrO_2	10	monoclinic (37-1484)	$a = 5.272$ $b = 5.151$ $c = 5.126$	230

[a] After calcination in a muffle furnace at 900 °C for 6 h. [b] Recalculated from the experimental XRD pattern.

Temperature-Programmed Reduction. Experiments were carried out in a conventional apparatus already described in a previous study.[28] An amount of 0.25 g of oxide is first prereduced at room temperature. The TPR itself proceeds by injection of CO pulses every 3 min into the He flow (30 mL min^{-1}). At the same time, the sample is heated from room temperature up to 600 °C at a ramp rate of 1.6 °C min^{-1}. Unconverted CO and produced CO_2 are analyzed with a gas chromatograph equipped with a Porapak Q column and a thermal conductivity detector (TCD).

The reducibility of the oxide is approached by calculating the total CO consumption (in μmol CO g^{-1}) or CO_2 formation.

Oxygen Storage Capacity. OSC of $Ce_xZr_{(1-x)}O_2$ samples were measured at 400 °C using the same kind of equipment as for TPR experiments. The sample (0.02 g) is first brought to 400 °C under flowing He (30 mL min^{-1}) before pretreatment under O_2. Injection of pulses of CO (0.267 mL) every 2 min up to a maximum reduction of the sample (10 pulses) is followed by five pulses of O_2. The cumulative oxygen storage capacity (OSCC) is calculated from both CO and O_2 uptake. This value characterizes the total amount of oxygen available in the oxide. After that, to simulate lean and rich working conditions of an engine, alternate pulses of CO or O_2 are injected. That way, we probed the amount of O_2 immediately available in these materials (OSC).

Oxygen storage capacities (OSCC and OSC) are expressed in μmol CO g^{-1} from the CO consumption or CO_2 formation (after CO pulses) or in μmol O g^{-1} from the O_2 consumption (O_2 pulses).

$C^{16}O$ Oxidation and Exchange. Experiments were carried out in a recycled reactor coupled to a mass spectrometer (QMG 420 Balzers). Mobile oxygen atoms of the oxide are first exchanged by contacting the sample with 50 mbar (1 mbar = 100 Pa) of $^{18}O_2$ at 400 °C for 2 h before 1 h outgassing at the same temperature. Carbon monoxide (50 mbar) is introduced in the reactor kept at 400 °C. Evolution of the isotopomer partial pressures of CO ($C^{16}O$, $C^{18}O$) and CO_2 ($C^{16}O_2$, $C^{18}O_2$, $C^{16}O^{18}O$) is monitored as a function of time.[29]

$^{18}O_2$ Isotopic Exchange. Experimental Procedure. Six oxides (CeO_2, $Ce_{0.68}Zr_{0.32}O_2$, $Ce_{0.63}Zr_{0.37}O_2$, $Ce_{0.50}Zr_{0.50}O_2$, $Ce_{0.15}Zr_{0.85}O_2$, and ZrO_2) were studied in the isotopic exchange of oxygen in order to examine the oxygen surface mobility. Experiments were carried out in the same equipment as for $C^{16}O$ oxidation and exchange on ^{18}O-preoxidized samples. A quantity of 2.5 m^2 of sample is placed in a quartz reactor and submitted to an in situ pretreatment proceeding as follows: oxidation ($^{16}O_2$) at 450 °C for 15 min; reduction (H_2) at 450 °C for 15 min; outgassing at 450 °C for 30 min. Finally, the sample is cooled to room temperature before reaction. Keeping in mind that all samples were supplied after precalcination at 900 °C for 6 h, which clearly allows the removal of nitrates and carbonates surface contaminants issuing from the preparation,[30] this optimized procedure is sufficient for cleaning the surface from atmospheric pollutants. The validity of this standard cleaning procedure was also ascertained during FT-IR studies.

Exchange starts with the introduction of 50 mbar of pure $^{18}O_2$ into the reactor. The temperature is increased from 25 to 600 °C at a ramp rate of 2 °C min^{-1}. Oxygen isotopomer partial pressures P_{32} ($^{16}O_2$), P_{34} ($^{16}O^{18}O$), and P_{36} ($^{18}O_2$) are sampled every 10 s.

Results Interpretation. From the variation in partial pressures, information on the rate of exchange (R_e), the number of oxygen exchanged (N_e), and the type of exchange mechanism may be obtained.[26]

$$R_e = -N_g \frac{d\alpha_g^t}{dt}$$

$$N_e = (\alpha_g^0 - \alpha_g^t)N_g$$

where N_g is the total number of oxygen atoms in the gas phase, α_g^t is the atomic fraction of oxygen-18 in the gas phase at time t, and α_g^0 is the initial atomic fraction of oxygen-18 in the gas phase.

Mechanisms for exchange are described by the following equations:[31]

simple heteroexchange:

$$^{18}O^{18}O_{(g)} + {}^{16}O_{(s)} \leftrightarrow {}^{18}O^{16}O_{(g)} + {}^{18}O_{(s)}$$

multiple heteroexchange:

$$^{18}O^{18}O_{(g)} + {}^{16}O^{16}O_{(s)} \leftrightarrow {}^{16}O_2 + {}^{18}O^{18}O_{(s)}$$

In our case, simple and multiple heteroexchange mechanisms are differentiated at the beginning of the reaction by prior appearance in the gas phase of $^{18}O^{16}O$ or $^{16}O_2$, respectively.

Results and Discussion

Oxygen Storage Capacity. OSCC and OSC are measured on cerium−zirconium mixed oxides calcined at 900 °C. OSCC values, obtained at 400 °C for all $Ce_xZr_{(1-x)}O_2$ samples (except ZrO_2), are reported in Table 2. Those results clearly show that the introduction of small amounts of zirconium in the CeO_2 lattice greatly improves its capacity to store oxygen and enhance its reductibility.

TABLE 2: OSC of $Ce_xZr_{(1-x)}O_2$ Mixed Oxides at 400 °C

	$Ce_xZr_{(1-x)}O_m$									
	CeO_2		$Ce_{0.68}Zr_{0.32}O_2$		$Ce_{0.63}Zr_{0.37}O_2$		$Ce_{0.50}Zr_{0.50}O_2$		$Ce_{0.15}Zr_{0.85}O_2$	
reduction[a]−oxidation[b] cycle	CO[a]	O_2[b]	CO[a]	O_2[b]	CO[a]	O_2[b]	CO[a]	O_2[b]	CO[a]	O_2[b]
cycle 1	76	126	198	603	201	598	160	586	34	103
cycle 2	17	1	113	1	105	2	87	2	17	1
cycle 3	10	0	72	1	69	1	58	2	13	0
Σ(cycles 4−10)	9	0	147	0	210	1	235	0	35	0
total OSCC	112	127	530	605	585	602	540	590	99	104
measured *m*	1.98		1.92		1.91		1.92		1.99	

[a] Reduction with CO uptake (μmol CO/g). [b] Oxidation with O_2 uptake (μmol O/g).

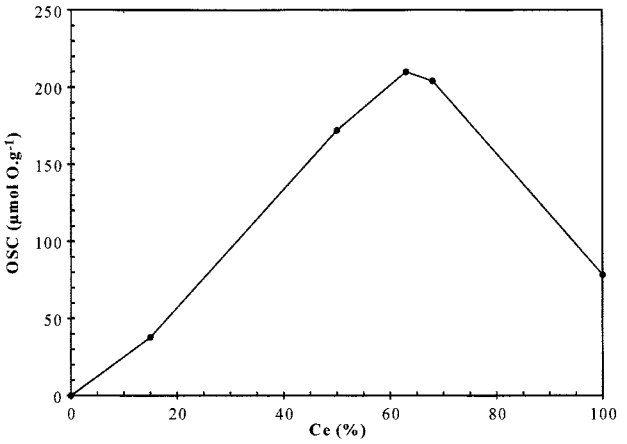

Figure 1. Oxygen storage capacity (μmol O g^{-1}) of $Ce_xZr_{(1-x)}O_2$ samples at 400 °C.

During OSCC measurements, CO uptake on an oxidized sample slowly decreases as the number of injected pulses increases. This observation indicates the kinetics of reduction. Nevertheless, after 10 pulses of CO, the sample is saturated and can be considered as "fully" reduced. In contrast, the reduced catalyst is completely reoxidized by the first pulse of O_2. This observation remains valid for all oxides. As a conclusion, the reduction of these oxides is much slower than their reoxidation.

Furthermore, on pure ceria, more CO is consumed compared to the amount of CO_2 produced. This discrepancy is attributed to the formation of carbonates species by reaction of CO with surface dioxygen species.[32−34] In fact, those species were clearly identified by FT-IR (1200−1600 cm^{-1}).

Figure 1 represents the variations of the OSC values vs cerium content. As already seen above, incorporation of zirconium into the CeO_2 lattice greatly improves the OSC. The largest OSC is obtained for $Ce_{0.63}Zr_{0.37}O_2$ with 219 μmol O g^{-1} (5.5 μmol O m^{-2}).

To go further into the interpretation of the results, the number of surface oxygen atoms may be calculated from the structure and the molar composition of the oxide (see Table 3). In what follows we will assume that Zr atoms do not participate in the redox process, no zirconium segregation occurs at the surface, and only one oxygen atom out of four is involved in the Ce^{4+}/Ce^{3+} reduction process. Furthermore, different orientations of the surface may be considered and we will base our comments assuming either a (100) or an average (100) + (110) + (111) surface. In recent papers, Hori et al.[35,36] simply considered a (100) surface.

In the case of CeO_2, OSC is limited to 74 μmol O g^{-1} (3 μmol O m^{-2}) and the number of surface oxygen atoms can be estimated to be 13.7 atoms nm^{-2} (cubic structure: a, b, c = 5.403 Å, (100) surface), corresponding to a theoretical OSC of 5.7 μmol O m^{-2}. Therefore, the storage of oxygen on ceria at 400 °C is restricted to the surface.

In the same way, for $Ce_{0.63}Zr_{0.37}O_2$, the number of surface oxygen atoms is estimated to be 14.2 atoms nm^{-2} (cubic structure: a, b, c = 5.31 Å, (100) surface) with a theoretical OSC of 3.7 μmol O m^{-2} while OSC measurements gave 5.5 μmol O m^{-2}. In that case, oxygen storage takes place not only at the surface but also in the bulk.

No change in the interpretations occurs when considering an average (100) + (110) + (111) surface instead of the (100) surface.

These results show that the introduction of small amounts of zirconium into the CeO_2 lattice promotes oxygen mobility. This specific behavior of mixed oxides is attributed to the participation of bulk oxygen atoms in the storage process.

In fact, similar results are found in the literature. Trovarelli et al.[7] studied oxygen storage (OSC) on $Ce_xZr_{(1-x)}O_2$ solid solutions prepared by mechanical milling of the parent oxides (ceria and zirconia). The maximum O_2 uptake was observed for solids with $0.6 \leq x \leq 0.8$, with an OSCC at 377 °C of approximately 185 μmol O_2 g^{-1}. The same trend was also observed by Cuif et al.[6,37] with an optimum OSC for $Ce_{0.6}Zr_{0.4}O_2$.

Temperature-Programmed Reduction. This method of characterization is used to test the reducibility of $Ce_xZr_{(1-x)}O_2$ solids. CO TPR measurements were carried out on oxides calcined at 900 °C. The results are shown in Figure 2. Reduction of CeO_2 by CO occurs from 200 °C and at a constant rate (constant CO consumption) up to higher temperature. The same type of flat profile had first been reported by Padeste et al. as they studied CO TPR of ceria.[38] In our case, the absence of any features at elevated temperature, presented as indicative of crystalline defects, could be taken as additional proof for the high perfection of the fluorite type structure of our ceria sample. For $Ce_xZr_{(1-x)}O_2$ with x = 0.15, 0.5, 0.63, and 0.68, one single peak is observed with maximum CO consumption around 570, 480, 470, and 450 °C, respectively. The CO uptake is much more important than for pure CeO_2.

At 400 °C, the cumulative CO uptake for CeO_2 and $Ce_xZr_{(1-x)}O_2$ is in agreement with OSC measurement results. In the case of pure ceria, reduction is restricted to the surface. At 600 °C, the cumulative CO consumption indicates that the reduction occurs both at the surface and in the bulk for all oxides. In fact, considering a (100) surface, the reduction reaches up to two and seven oxygen atoms layers for CeO_2 and $Ce_{0.63}Zr_{0.37}O_2$, respectively.

By substitution of Ce^{4+} by Zr^{4+}, the reducibility of the solids is widely modified. Cerium−zirconium mixed oxides are much more reducible than CeO_2. The same conclusions were also drawn from previous H_2 TPR. In fact, H_2 uptake on $Ce_xZr_{(1-x)}O_2$ samples has been widely studied.[4,7,39,40] All the results show that incorporation of zirconium in the CeO_2 lattice greatly

TABLE 3

oxide $Ce_xZr_{(1-x)}O_2$	structure	total number of surface oxygen atoms (atoms nm^{-2}) theoretical OSC (μmol O m^{-2})[a] (100)[b]	(110)[c]	(111)[d]	(100) + (110) + (111)[e]
CeO_2	cubic	13.7	9.7	15.8	13.1
		5.7	4.0	6.6	5.4
$Ce_{0.68}Zr_{0.32}O_2$	cubic	14.1	10.0	16.3	13.5
		4.0	2.8	4.6	3.8
$Ce_{0.63}Zr_{0.37}O_2$	cubic	14.2	10.0	16.4	13.5
		3.7	2.6	4.3	3.5
$Ce_{0.50}Zr_{0.50}O_2$	tetragonal[f]	14.4	10.2	16.6	13.7
		3.0	2.1	3.5	2.9
$Ce_{0.15}Zr_{0.85}O_2$	tetragonal[f]	15.1	10.7	17.4	14.4
		0.9	0.7	1.1	0.9

[a] Considering that zirconium atoms do not participate in the storage process, no zirconium segregation occurs at the surface, and only one atom out of four is involved in the process (CeO_2/Ce_2O_3). [b] (100) surface, cubic structure: four atoms, located at (a/4) out of the Ce plan, in (a^2). [c] (110) surface, cubic structure: four atoms, located in the plan, in ($a^2/\sqrt{2}$). [d] (111) surface, cubic structure: two atoms, located ($a/(3\sqrt{3})$ out of the plan, in ($a^2\sqrt{3}/4$). [e] Average (equidistribution of the three planes). [f] For the calculations, the tetragonal cell was assumed to be a homothetic distortion of the cubic cell. The above formula was transposed to the tetragonal system with $a,b_{\text{tetragonal}} = a,b_{\text{cubique}}\sqrt{2}$.

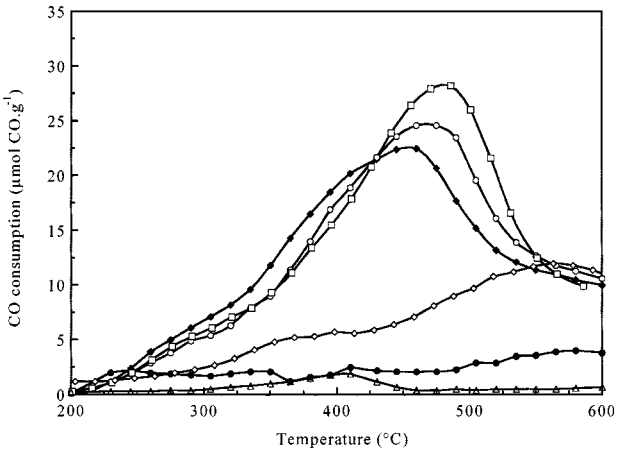

Figure 2. CO consumption calculated from TPR of $Ce_xZr_{(1-x)}O_2$: (●) CeO_2; (◆) $Ce_{0.68}Zr_{0.32}O_2$; (○) $Ce_{0.63}Zr_{0.37}O_2$; (□) $Ce_{0.0.50}Zr_{0.50}O_2$; (◇) $Ce_{0.15}Zr_{0.85}O_2$, (△) ZrO_2.

increases the H_2 consumption and decreases the temperature of bulk reduction. For pure CeO_2, two peaks are observed around 600 and 800 °C corresponding to the reduction of the surface and the bulk, respectively.[41,42] In the case of mixed oxides, the second peak is shifted toward lower temperatures and the far larger H_2 uptake indicates a deeper reduction.

$C^{16}O$ Oxidation and Exchange. $C^{16}O$ oxidation and exchange was investigated on ^{18}O-preoxidized CeO_2 and $Ce_{0.63}Zr_{0.37}O_2$ in order to understand the reactivity of surface oxygen atoms. These reactions also give additional information on the oxygen availability. In fact, this method had already been successfully used for the study of surface oxygen exchange reactions on Rh/CeO_2 catalysts.[43]

Evolution of the partial pressures for both $C^{16}O$ and the various products is recorded as a function of time. Results are shown in Figure 3 for CeO_2 and $Ce_{0.63}Zr_{0.37}O_2$. For both samples, oxidation of $C^{16}O$ to $C^{16}O_2$ is the predominant reaction while the formation of $C^{18}O_2$ is rarely detected. Moreover, exchange of $C^{16}O$ to $C^{18}O$ may be observed at a very low level. On $Ce_{0.63}Zr_{0.37}O_2$, the oxidation of $C^{16}O$ to $C^{16}O_2$ occurs much more quickly than on CeO_2. Oxygen is then much more mobile in this mixed oxide than in ceria.

To go further in the interpretation, the oxidation reaction can be written as

$$CO + O_s \xrightarrow{k} CO_2$$

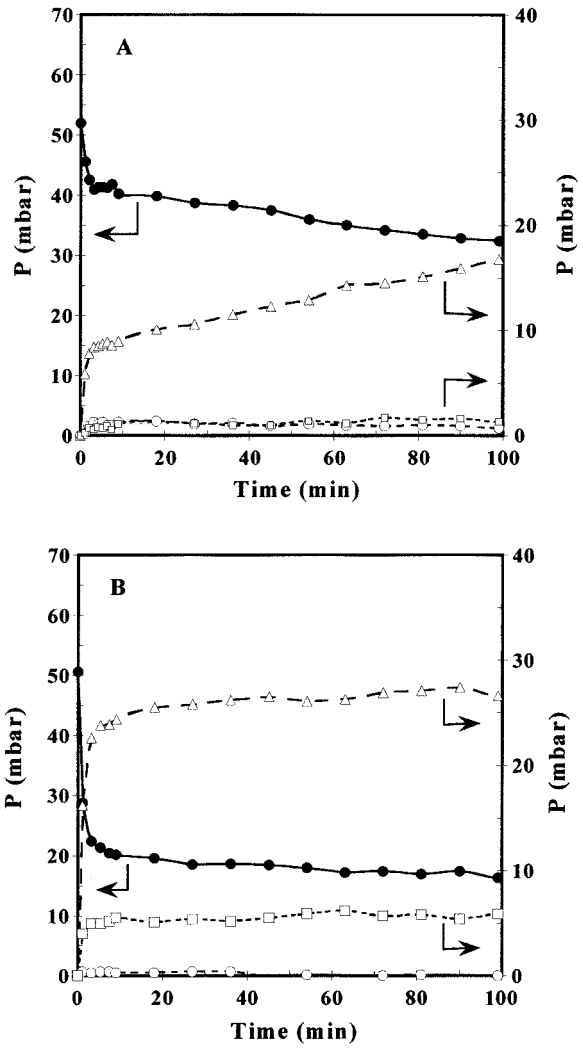

Figure 3. Evolution of the isotopomer partial pressures of CO (●, $C^{16}O$; ○, $C^{18}O$) and CO_2 (△, $C^{16}O_2$; □, $C^{16}O^{18}O$) as a function of time during $C^{16}O$ oxidation and exchange on CeO_2 (A) and on $Ce_{0.63}Zr_{0.37}O_2$ (B). Samples are preexchanged by $^{18}O_2$ at 400 °C.

with r the rate of transformation of $C^{16}O$,

$$r = kP_{CO}[O_s]$$

Assuming steady-state conditions, the rate of transformation of CO is then directly equal to the rate of formation of CO_2:

$$-\frac{d[CO]}{dt} = \frac{d[CO_2]}{dt}$$

with

$$\frac{d[CO_2]}{dt}$$

proportional to P_{CO_2}. Furthermore, if we assume that all reacting CO gives $CO_{2(g)}$ and that all formed CO_2 comes from $CO_{(g)}$, the only possible reactions are

$$C^{16}O + {}^{16}O_s \xrightarrow{k} C^{16}O_2$$

$$C^{16}O + {}^{18}O_s \xrightarrow{k} C^{16}O^{18}O$$

$$C^{18}O + {}^{16}O_s \xrightarrow{k} C^{16}O^{18}O$$

Starting from these reactions and by combining the different reaction rates, we get

$$\alpha = \frac{P_{C^{16}O} - xP_{C^{18}O}}{P_{C^{16}O}(x+1) - xP_{C^{18}O}}$$

where

$$x = \frac{P_{C^{16}O_2}}{P_{C^{16}O^{18}O}}$$

with $P_{C^{16}O}$, $P_{C^{18}O}$, $P_{C^{16}O^{18}O}$ being the $C^{16}O$, $C^{18}O$, and $C^{16}O^{18}O$ partial pressures, respectively, and α being the fraction of ^{18}O atoms on the catalyst surface. From the early evolution of the partial pressures, α was calculated for both CeO_2 and $Ce_{0.63}Zr_{0.37}O_2$. We obtained $\alpha = 0.05$ and 0.19 for CeO_2 and $Ce_{0.63}Zr_{0.37}O_2$, respectively. Now, from the results above we also know that during this period only surface oxygen atoms are involved in CO oxidation. Then the number of surface ^{18}O sites on $Ce_{0.63}Zr_{0.37}O_2$ participating in CO oxidation is 4 times greater than on CeO_2. This difference can be explained by the difference in the amplitude of the exchange during the ^{18}O pretreatment. In fact, we saw earlier, from the OSC measurements, that mixed oxides were able to store 4 times more oxygen than pure ceria.

Both methods (CO oxidation on ^{18}O-preoxidized samples and the OSC measurements) are in very good agreement. Then a simple measure of the OSC already gives a good indication on the storage properties of the material.

$^{18}O_2$ Isotopic Exchange. Cerium−zirconium mixed oxides and ceria exchange in a narrow range of temperatures (Figure 4A). The temperature at the maximum rate of exchange (T_{max}) varies between 440 and 540 °C. As zirconium content increases, T_{max} is progressively moved to higher temperature and the maximum rate of exchange increases. This surprising observation could be explained by the increase in the amount of oxygen exchanged. In the case of pure ZrO_2, $^{18}O_2$ exchange only occurs at elevated temperature (T_{max} = 570 °C). As a conclusion, the introduction of zirconium into the CeO_2 lattice favors the exchange.

For all oxides the total number of oxygen atoms exchanged at 600 °C (30−45 atoms nm^{-2}) is important and much larger than the calculated number of surface oxygens (10−17 atoms nm^{-2}) (Figure 4B). In fact, for CeO_2 and $Ce_{0.63}Zr_{0.37}O_2$ oxides, surface oxygen atoms are already totally exchanged by 400 °C. More precisely, from Table 4 we can see that this process also involves bulk oxygen atoms, with up to three oxygen layers

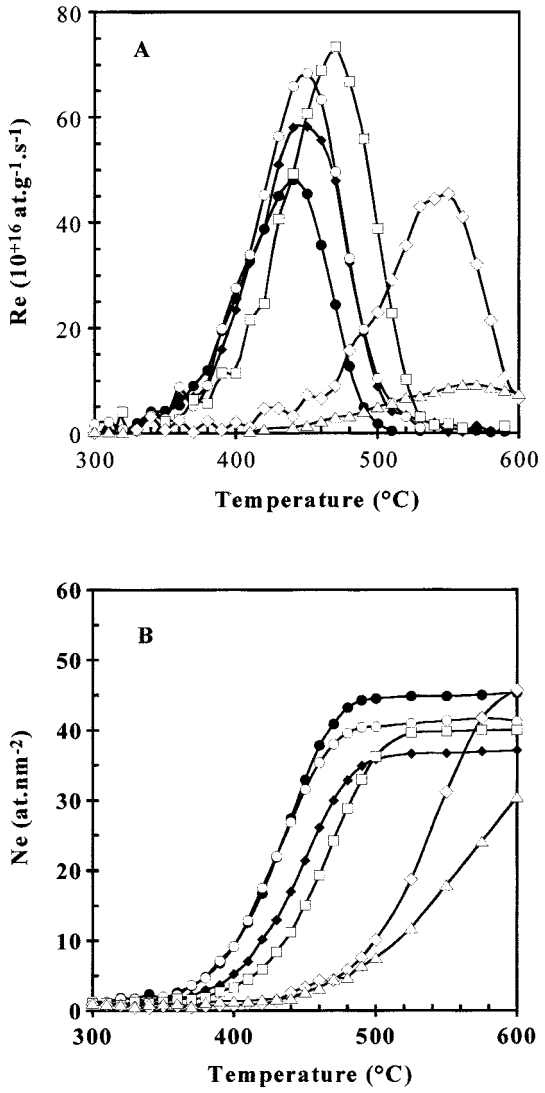

Figure 4. Evolution of the rate of oxygen exchange R_e (A) and number of oxygen atoms exchanged N_e (B) on $Ce_xZr_{(1-x)}O_2$ solids as a function of temperature (●, CeO_2; ◆, $Ce_{0.68}Zr_{0.32}O_2$; ○, $Ce_{0.63}Zr_{0.37}O_2$; □, $Ce_{0.50}Zr_{0.50}O_2$; ◇, $Ce_{0.15}Zr_{0.85}O_2$; △, ZrO_2).

exchanged (N_l). Again, $Ce_{0.63}Zr_{0.37}O_2$ is the most reactive sample toward O_2, as already seen before from OSC measurements.

To identify the kind of mechanism of exchange on these oxides, the variation of P_{32} and P_{34} versus temperature was plotted (Figure 5). On CeO_2, a simultaneous evolution of the partial pressures in $^{16}O_2$ (P_{32}) and $^{18}O^{16}O$ (P_{34}) is observed at the beginning of the exchange (Figure 5A). This observation implies that both simple and multiple mechanisms take place at the same time. In the case of ZrO_2, $^{18}O^{16}O$ is the first to be observed in the gas phase, which indicates a simple heteroexchange. For all mixed oxides, both simple and multiple mechanisms are observed (Figure 5B). Nevertheless, multiple heteroexchange is much more predominant on $Ce_xZr_{(1-x)}O_2$ at the very beginning of the exchange (between 380 and 440 °C) than it is on pure ceria.

Additional investigations on CeO_2 and $Ce_{0.68}Zr_{0.32}O_2$ were made on reduced and oxidized samples in order to study the effect of pretreatment. These experiments were carried out with 50 mbar of $^{18}O_2$. We reported the variation of the ratio P_{32}/P_{34} versus temperature (Figure 6). When P_{32}/P_{34} is less than 1, simple heteroexchange is predominant, while multiple heteroexchange is favored for P_{32}/P_{34} greater than 1. For CeO_2, multiple heteroexchange is more favored on prereduced than preoxidized

TABLE 4: Temperature-Programmed Isotopic Exchange of $^{18}O_2$ on Prereduced Oxides

oxides	exchange temperature range (°C)	temperature at R_e max (T_{max}) (°C)	R_e max (10^{+16} at $g^{-1}.s^{-1}$)	mechanism of exchange[a]	N_e total[b] (atoms nm^{-2})	N_l[c]
CeO_2	310−510	440	48	S + M	45.3	3.3
$Ce_{0.68}Zr_{0.32}O_2$	310−550	445	58	S + M	37.1	2.6
$Ce_{0.63}Zr_{0.37}O_2$	330−530	450	68	S + M	41.2	2.9
$Ce_{0.50}Zr_{0.50}O_2$	350−560	470	73	S + M	40.0	2.2
$Ce_{0.15}Zr_{0.85}O_2$	370−610	540	45	S + M	49.3	3.3
ZrO_2	410−810	570	9	S	30.4	2

[a] Mechanism of exchange: simple (S) and multiple (M). [b] Total number of oxygen atoms exchanged up to 600 °C. [c] Number of oxygen layers exchanged up to 600 °C considering a (100) surface.

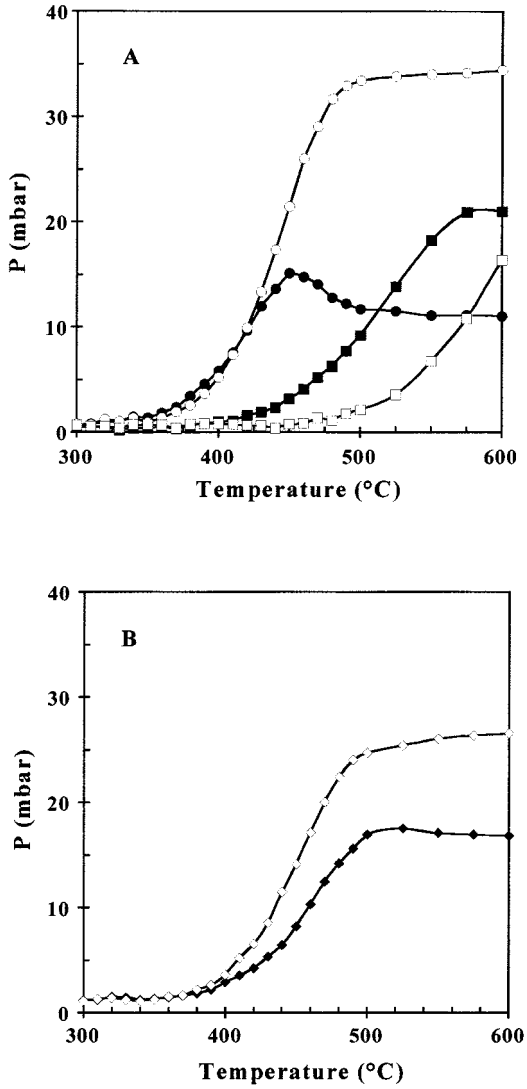

Figure 5. Variations of oxygen isotopomers partial pressures during $^{18}O_2$ TPIE: (A) on CeO_2 (●, ○) and ZrO_2 (■, □); (B) on $Ce_xZr_{(1-x)}O_2$ (◆, ◇); (open symbols) $^{16}O_2$; (full symbols) $^{16}O^{18}O$. Oxides are prereduced under H_2 at 450 °C for 15 min.

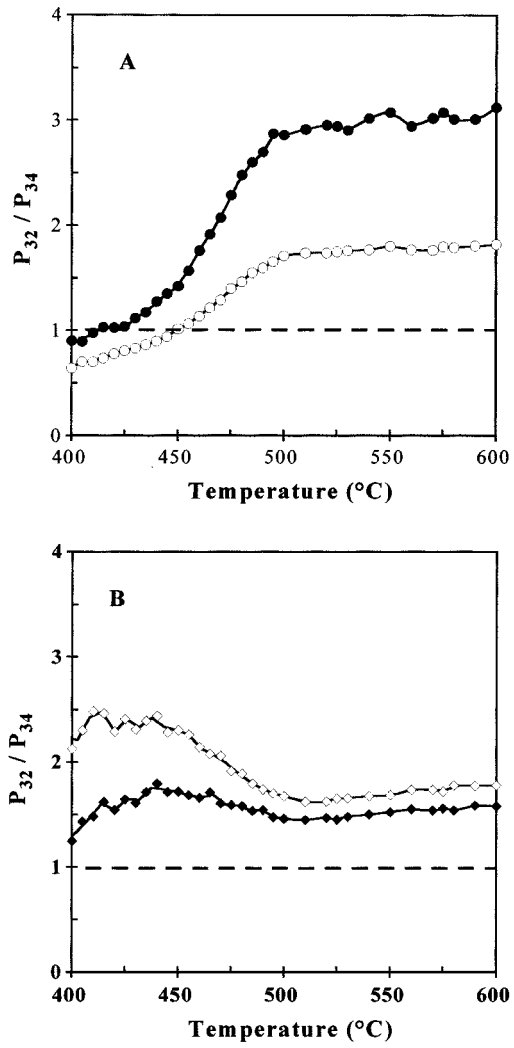

Figure 6. Evolution of the partial pressure ratio P_{32}/P_{34} as a function of temperature during TPIE experiments on CeO_2 (A) and $Ce_{0.68}Zr_{0.32}O_2$ (B). Effect of the pretreatment is shown for reduction under H_2 at 450 °C for 15 min (full symbols) or oxidation under O_2 at 450 °C for 15 min (open symbols).

samples (Figure 6A). In contrast, for $Ce_{0.68}Zr_{0.32}O_2$, the multiple mechanism is more predominant after an oxidizing pretreatment (Figure 6B). Pretreatment effects could be related to the variation in surface oxygen species populations.

Multiple heteroexchange occurs with simultaneous participation of two oxygen atoms of the oxide. Surface dioxygen intermediates involved could be superoxides (O_2^-) or peroxides (O_2^{2-}) as proposed by Yao et al.[1] Li et al.[44,45] studied dioxygen adsorption on ceria using FT-IR spectroscopy. Superoxides are indicated by a band at 1126 cm^{-1} and were found to be very sensitive to the pretreatment. Peroxide species are observed only on prereduced samples and identified by a band at 883 cm^{-1}.

In our case, dioxygen adsorption was investigated by FT-IR spectroscopy on both ceria and $Ce_xZr_{(1-x)}O_2$ mixed oxide. Results obtained after oxidation of the wafer are shown in Figure 7. One minute after admission of O_2 at room temperature, one single band at 1126 cm^{-1}, characteristic of superoxides, is observed.

In the case of mixed oxides, the intensity of this band is also affected by the pretreatment of the sample. In fact, after a reducing treatment, the integrated surface of the band at 1126 cm^{-1} is lowered. This observation exactly correlates with the beginning of exchange presented above. The predominance of the multiple heteroexchange after an oxidizing treatment is

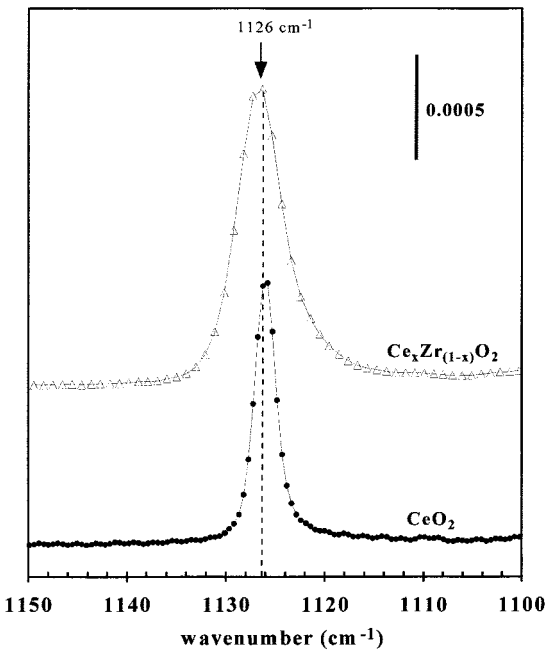

Figure 7. IR spectra of adsorbed dioxygen on preoxidized CeO_2 and $Ce_xZr_{(1-x)}O_2$ 1 min after admission of 20 mbar O_2 at 25 °C (absorbance m^{-2}).

derived from the higher concentration in superoxides at the surface. Furthermore, the large predominance of multiple heteroexchange at the beginning of the exchange on mixed oxides compared to pure ceria could be related to the presence at the surface of larger concentrations of dioxygen species (superoxides and peroxides), as indicated by FT-IR spectroscopy.

For CeO_2, such a correlation has not yet been possible. In fact, carbonates species were also detected with specific bands in the 1300−1400 cm^{-1} wavenumber range.[46] Thus, since dioxygen species may be trapped to form carbonates by reaction with residual carbon, a proper quantification of superoxide species is difficult. To succeed, an extremely clean surface is required.

Furthermore, more recently, dioxygen adsorption on $Ce_xZr_{(1-x)}O_2$ prepared by a sol−gel process[8] has been investigated by Rossignol et al.[47] A successful correlation between OSC and the amount of surface dioxygen species observed by FT-IR was possible.

Conclusions

A study of monophasic zirconium−cerium mixed oxides ($Ce_xZr_{(1-x)}O_2$, $0 \leq x \leq 1$) demonstrated their specific properties.

First of all, Ce^{4+}/Zr^{4+} cation isomorphous substitution in the ceria lattice markedly improves the thermal stability of such prepared oxides. In fact, after calcination at 900 °C, Ce-rich mixed oxides maintain a relatively high surface area (40−50 $m^2\ g^{-1}$) compared to pure ceria. This makes those new materials good supports for catalytic converters.

Furthermore, oxygen storage capacity, redox properties, and oxygen mobility are also positively modified. In fact, OSC measurements and TPR experiments showed for Ce-rich mixed oxides both better oxidizing and better reducing abilities with larger OSC and CO uptake, respectively. In the same way, oxygen isotopic exchange studies indicated that mixed oxides react more quickly and on a larger scale than pure ceria. An optimum was identified for $Ce_{0.63}Zr_{0.37}O_2$ with an OSC at 400 °C of 219 μmol O g^{-1}.

Finally, when TPIE results (number of exchanged atoms, exchange mechanism, ...) were closely examined, the behavior of $Ce_xZr_{(1-x)}O_2$ was attributed to the participation of bulk oxygen atoms (number of oxygen layers exchanged was ∼3) and dioxygen surface species (superoxides, peroxides).

References and Notes

(1) Yao, H. C.; Yu Yao, Y. F. *J. Catal.* **1984**, *86*, 254.
(2) European Patent EP 337809, 1989.
(3) Ozawa, M.; Kimura, M.; Isogai, A. *J. Alloys Compd.* **1993**, *193*, 73.
(4) Murota, T.; Hasegawa, T.; Aozasa, S.; Matsui, H.; Motoyama, M. *J. Alloys Compd.* **1993**, *193*, 298.
(5) Ranga, R.; Kašpar, J.; Di Monte, R.; Meriani, S.; Graziani, M. *Catal. Lett.* **1994**, *24*, 107.
(6) Cuif, J. P.; Blanchard, G.; Touret, O.; Seigneurin, A.; Marczi, M.; Quemere, E. Presented at SAE (Society of Automotive Engineers), Paper 970463, 1997.
(7) Trovarelli, A.; Zamar, F.; Llorca, J.; De Leitenbourg, C.; Dolcetti, G.; Kiss, J. T. *J. Catal*. **1997**, *169*, 490.
(8) Rossignol, S.; Madier, Y.; Duprez, D. *Catal. Today* **1999**, *50*, 261.
(9) Kašpar, J.; Fornasiero, P.; Graziani, M. *Catal. Today* **1999**, *50*, 285.
(10) Hirata, T.; Zhu, H.; Furubayashi, T.; Nakatani, I. *J. Am. Ceram. Soc*. **1993**, *76* (5), 1361.
(11) Torng, S.; Miyazawa, K.; Sakuma, T. *Mater. Sci. Technol.* **1995**, *11*, 130.
(12) Yashima, M.; Morimoto, K.; Ishizawa, N.; Yoshimura, M. *J. Am. Ceram. Soc*. **1993**, *76* (11), 2865.
(13) Yashima, M.; Ohtake, K.; Kakihana, M.; Yoshimura, M. *J. Am. Ceram. Soc*. **1994**, *77* (10), 2773.
(14) Tsukuma, K. *Am. Ceram. Soc. Bull*. **1986**, *65* (10), 1386.
(15) Yashima, M.; Morimoto, K.; Ishizawa, N.; Yoshimura, M. *J. Am. Ceram. Soc*. **1993**, *76* (7), 1745.
(16) Meriani, S. *Mater. Sci. Eng*. **1989**, *109*, 121.
(17) Kim, D. J.; Jung, H. J.; Kim, H. J. *J. Mater. Sci. Lett*. **1995**, *14*, 285.
(18) Zhu, H. V. *J. Mater. Sci*. **1994**, *29*, 4351.
(19) Vlaic, G.; Fornasiero, P.; Geremia, S.; Kašpar, J.; Graziani, M. *J. Catal*. **1997**, *168*, 386.
(20) Vlaic, G.; Di Monte, R.; Fornasiero, P.; Fonda, E.; Kašpar, J.; Graziani, M. *Stud. Surf. Sci. Catal*. **1997**, *116*, 73.
(21) Yashima, M.; Arhashi, H.; Kakihana, M.; Yoshimura, M. *J. Am. Ceram. Soc*. **1994**, *77* (4), 1067.
(22) Yao, M. H.; Baird, R. J.; Kung, F. W.; Hoost, T. E. *J. Catal*. **1997**, *166*, 67.
(23) Fornasiero, P.; Balducci, G.; Di Monte, R.; Kašpar, J.; Meriani, S.; Trovarelli, A.; Graziani, M. *Catal. Today* **1996**, *29*, 47.
(24) Fornasiero, P.; Di Monte, R.; Ranga Rao, G.; Kašpar, J.; Meriani, S.; Trovarelli, A.; Graziani, M. *J. Catal*. **1995**, *151*, 168.
(25) Balducci, G.; Fornasiero, P.; Di Monte, R.; Kašpar, J.; Meriani, S.; Graziani, M. *Catal. Lett.* **1995**, *33*, 193.
(26) Martin, D.; Duprez, D. *J. Phys. Chem*. **1996**, *100*, 9426.
(27) Martin, D. Ph.D. Thesis, University of Poitiers, Poitiers, France, 1994.
(28) Duprez, D. *J. Chim. Phys*. **1983**, *80*, 487.
(29) Taha, R.; Martin, D.; Kacimi, S.; Duprez, D. *Catal. Today* **1996**, *29*, 89.
(30) Daturi, M.; Binet, C.; Lavalley, J. C.; Vidal, H.; Kašpar, J.; Graziani, M.; Blanchard, G. *J. Chim. Phys.* **1998**, *95*, 2048.
(31) Boreskov, G. K. *Adv. Catal*. **1964**, *15*, 285.
(32) Li, C.; Sakata, Y.; Arai, T.; Domen, K.; Maruya, K. I.; Onishi, T. *J. Chem. Soc., Faraday Trans*. **1989**, *85* (4), 929.
(33) Li, C.; Sakata, Y.; Arai, T.; Domen, K.; Maruya, K. I.; Onishi, T. *J. Chem. Soc., Faraday Trans*. **1989**, *85* (6), 1451.
(34) Binet, C.; Badri, A.; Boutonnet, K. M.; Lavalley, J. C. *J. Chem. Soc., Faraday. Trans*. **1994**, *90* (7), 1023.
(35) Hori, C. E.; Permana, H.; Ng, K. Y. S.; Brenner, A.; More, K.; Rahmoeller, K. M.; Belton, D. *Appl. Catal. B* **1998**, *16*, 105.
(36) Hori, C. E.; Brenner, A.; Ng, K. Y. S.; Rahmoeller, K. M.; Belton, D. *Catal. Today* **1999**, *50*, 299.
(37) Cuif, J. P.; Blanchard, G.; Touret, O.; Marczi, M.; Quemere, E. Presented at SAE, Paper 961906, 1996.
(38) Padeste, C.; Cant, N. W.; Trimm, D. L. *Catal. Lett.* **1993**, *18*, 305.
(39) Fornasiero, P.; Balducci, G.; Di Monte, R.; Kašpar, J.; Sergo, V.; Gubitosa, G.; Ferrero, A.; Graziani, M. *J. Catal*. **1996**, *164*, 173.
(40) Fornasiero, P.; Kašpar, J.; Graziani, M. *J. Catal*. **1997**, *167*, 576.
(41) Trovarelli, A.; Dolcetti, G.; De Leitenburg, C.; Kašpar, J.; Finetti, P.; Santoni, A. *J. Chem. Soc., Faraday. Trans*. **1992**, *88* (9), 1311.

(42) De Leitenburg, C.; Trovarelli, A.; Kašpar, J. *J. Catal*. **1997**, *166*, 98.
(43) Taha, R.; Martin, D.; Kacimi, S.; Duprez, D. *Catal. Today* **1996**, *29*, 89.
(44) Li, C.; Domen, K.; Maruya, K.; Onishi, T. *J. Am. Chem. Soc*. **1989**, *111*, 7683.
(45) Li, C.; Domen, K.; Maruya, K.; Onishi, T. *J. Catal*. **1990**, *123*, 436.
(46) Soria, J.; Martinez-Arias, A.; Conesa, J. *J. Chem. Soc., Faraday Trans*. **1995**, *91* (11), 1669.
(47) Rossignol, S.; Gérard, F.; Duprez, D. *J. Mater. Chem*. **1999**, *9*, 1615.